Table 1
CT density of coronary artery soft plaque in literature.

Author	CT density (HU)	Species	Plaque (no.)	Scan	CT	DAS (no.)	Tube voltage (kV)	Analysis	Reference
Schroeder	14 ± 26 (−42 to 47)	Human	12	In vivo	MDCT	4	140	IVUS	[8]
Becker	47 ± 9	Human	21	Ex vivo	MDCT	4	120	Histology	[9]
Juan	51 ± 25	Rabbit	60	In vivo	MDCT	16	120	Histology	[10]
Leber	49 ± 22 (14 to 82)	Human	80	In vivo	MDCT	16	120	IVUS	[11]
Schroeder	42 ± 22 (22 to 58)	Human	6	Ex vivo	MDCT	4	140	Histology	[12]
Nikolaou	47 ± 13	Human	10	Ex vivo	MDCT	4	120	Histology	[13]
Rasouli	23 ± 71	Human	12	In vivo	e-Speed	20	130	IVUS	[14]
Pohle	58 ± 43 (−39 to 167)	Human	176	In vivo	MDCT	16	120	IVUS	[15]
Kitagawa	18 ± 17	Human	25	In vivo	MDCT	64	120	IVUS	[16]
Sun	79 ± 34 (7–149)	Human	NA	In vivo	MDCT	64	120–135[a]	IVUS	[17]

CT density in Hounsfield units (HU) is expressed as mean ± standard deviation (range); MDCT: multidetector computed tomography; DAS: detector array system; IVUS: intravascular ultrasound; NA: non-applicable.
[a] Tube voltage was modified depending on patient size.

axial coronary MDCTA in coronary artery soft plaque diagnosis.

2. Materials and methods

2.1. Cardiac phantom

We used a commercially available prototype cardiac phantom (Alpha 2, Fuyo Corporation). The phantom consisted of five components: driver, control, support, rubber balloon and ECG. A controller with an ECG-synchronizer drives the balloon. The main characteristics of this phantom are programmable variable heart rate sequences including arrhythmia. However, as this study aimed to investigate soft plaque visualization in different tube voltages, to avoid influence of excessive motion artifacts, low heart rates of 55 bpm, 50 bpm and 65 bpm were programmed.

2.2. Coronary artery soft plaque models

Coronary artery cylinder and soft plaque models were manufactured for this experiment (Fuyo corp. Tokyo, Japan). D-shaped stenosis, with angiographical stenosis levels of 25%, 50% and 75%, simulated soft plaques (Fig. 1). Following literature review, we prepared five kinds of soft plaque models, mimicking CT values (Tables 1 and 2). The coronary artery models, made of acrylonitrile–butadiene–styrene transparent (44 HU), were filled with four kinds of diluted contrast material (205 HU, 241 HU, 280 HU and 314 HU). These were attached to the balloon phantom (mimicking the heart) with the long axis of the model corresponding to the z-axis and were surrounded by corn oil (−122 HU) simulating epicardial fat (Table 2 and Fig. 2). This phantom construction simulated a slim human thorax regarding X-ray absorption and mimicked the image noise characteristics.

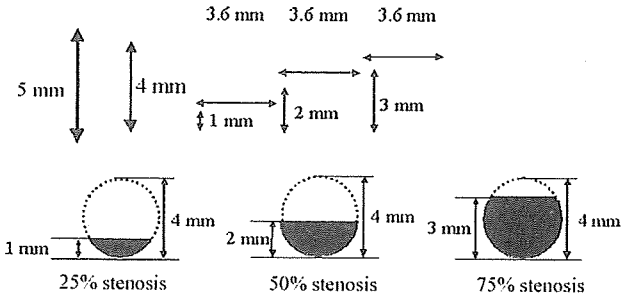

Fig. 1. Coronary artery and soft plaque models. This diagram shows a configuration of coronary artery models with an inner diameter of 4 mm. The artificial soft plaques are attached to the arterial wall. Stenosis of plaques was 25%, 50% and 75%.

Table 2
Densitometry of soft plaque and coronary artery models.

Material for soft plaque models	120 kV	100 kV
Acrylonitrile–butadiene–styrene white	−32	−42
Tough water phantom WE type (Kyoto Kagaku Co. Ltd.)	10	2
Polyphenylene oxide	36	5
Acrylonitrile–butadiene–styrene transparent	44	28
Nylon 6	53	44
Intracoronary enhancement 1	205	256
Intracoronary enhancement 2	241	296
Intracoronary enhancement 3	280	333
Intracoronary enhancement 4	314	376

Densitometry of all samples (plaque models and intracoronary enhancement) greater than 10 cm^2 was performed in corn oil at static state. CT values were mean of measurements ($n = 5$).

2.3. Prospective ECG-triggered coronary 64-slice CTA protocol

Prospective ECG-triggered coronary CTA was performed using a LightSpeed VCT (GE Healthcare, Waukesha, WI, USA). The tube voltage was 100 kV or 120 kV and the current was 650 mA. The X-ray pulsing window was set to the minimum (233 ms, 2/3 of the gantry rotation time). The prospective scan was performed so that the center of the temporal window corresponded to 80% of R–R

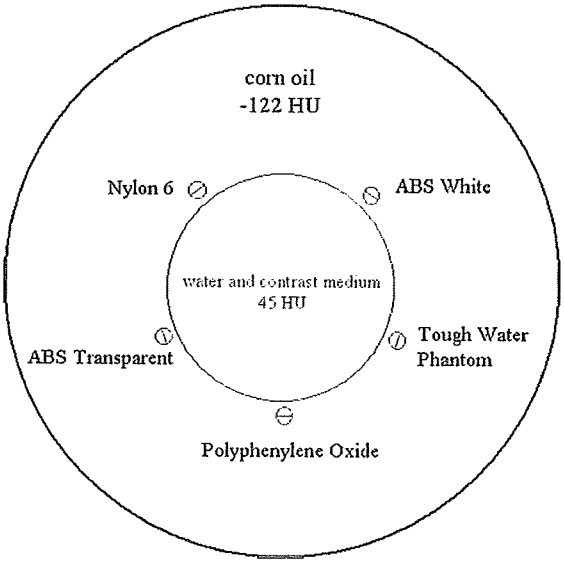

Fig. 2. Cardiac balloon phantom. The balloon was filled with a mixture of water and contrast medium (45 HU) to simulate weakly enhanced myocardium (at the arterial phase) and was submerged in corn oil (−122 HU), simulating epicardial and pericardial fat. Coronary artery models ($n = 5$) were attached to the balloon surface.

Please cite this article in press as: Horiguchi J, et al. In vitro measurement of CT density and estimation of stenosis related to coronary soft plaque at 100 kV and 120 kV on ECG-triggered scan. Eur J Radiol (2009), doi:10.1016/j.ejrad.2009.08.002

interval (diastole of the phantom). Half-segmented reconstruction algorithm with a standard reconstruction filter was used. The temporal resolution was 175 ms. The matrix size was 512 × 512 pixels and the display field of view was 12 cm. To pretest the image quality being eligible for quantitative analysis, multiplanar reformations (MPRs) parallel to the long axis of the coronary artery were created on a separate workstation (Advantage WorkStation Version 4.2, GE Healthcare).

2.4. Soft plaque density

Two independent observers (J.H., C.F., coronary CTA reading experience of 7 and 5 years) measured the density of soft plaque, using a standard region of interest (ROI, 2 mm^2) technique. A window level/width of 600/100 was used for visualization in the axial plane. Plaques with 50% stenosis were selected, as densitometry of small plaque is substantially affected by intracoronary enhancement [23] which might cover up the effect of tube voltage. The measurement was performed on three slices and the mean was obtained. The measurement (n = 60; 3 heart rate sequences × 5 plaques × 4 intracoronary enhancement) by two observers was correlated and the mean of the measurement (two means) was defined as 'soft plaque density'. The soft plaque density was compared between 100 kV and 120 kV scans and between plaques using repeated measures analysis of variance (ANOVA).

2.5. Measurement error of stenosis

Stenosis level of soft plaque was independently measured by two observers (J.H. and C.F.) using an electronic caliper in a zoomed image to ensure exact placement of the caliper. A window level/width of 600/100 was used for visualization in the axial plane. Per each stenosis level, the measurement was performed on three slices and the mean was obtained. The measurement (n = 180; 3 heart rate sequences × 5 plaques × 3 stenosis levels × 4 intracoronary enhancement) by two observers was correlated and the mean of the measurement (two means) was defined as 'stenosis level'. The measurement error of coronary artery stenosis was defined as *abs* (measured stenosis level − known stenosis level)/known stenosis level. The measurement errors were compared between 100 kV and 120 kV scans and between three stenosis levels.

2.6. Radiation dose

Volume computed tomography dose index (CTDIvol) displayed on the CT scanner was recorded on 100 kV and 120 kV scans. As dose-length product (DLP) displayed on the phantom study is not suited for simulating DLP on patients' scan, DLP is defined with the assumption that heart ranges 14 cm in the z-axis:

$$\mathrm{DLP\,(mGy \times cm)} = \mathrm{CTDIvol\,(mGy)} \times 14\,\mathrm{cm}$$

An approximation of the effective dose (E) can be obtained using the equation [24]:

$$E = k \times \mathrm{DLP}$$

where E is effective dose estimate and k = 0.017 $\mathrm{mSv\,mGy^{-1}\,cm^{-1}}$. This value is applicable to chest scans and is the average between the male and female models.

2.7. Statistical analysis

Statistical analysis was performed using the MedCalc statistical software (MedCalc 9.5.1 for Windows, Medcalc Software, Mariakerke, Belgium). Data are expressed as mean ± SD. Interobserver reliability for the measurement of density or stenosis was tested using Bland–Altman analysis and Pearson correlation coefficient with a 95% confidence interval (CI).

3. Results

All soft plaque models, with three stenosis levels, were clearly visualized in the study applying low heart rates, thereby were considered suitable for quantitative analysis. To illustrate, MPR images of soft plaque models on 65 bpm, under the lowest intracoronary enhancement of 205 HU, which are considered to be the most difficult conditions for plaque delineation, are shown (Fig. 3).

3.1. Soft plaque density

The measurement of soft plaque density is shown in Table 3. The interobserver correlation of the measurement was high (Pearson, r = 0.953, 95% CI: 0.933–0.967, $p < 0.01$). Although the density of all soft plaques (gross materials) in static state was lower at 100 kV than 120 kV (Table 2), there was no difference in the density between 100 kV and 120 kV on the simulation of coronary CTA (Fig. 4). The density on plaque and tube voltage considerably varied among measurements (n = 12, 3 heart rate sequences × 4 intracoronary enhancement) with standard deviation of the CT densitometry ranging 6 HU to 16 HU).

3.2. Measurement error of stenosis

The measurement of plaque stenosis is shown in Table 3. The interobserver correlation of the measurement was high (Pearson, r = 0.975, 95% CI: 0.969–0.980, $p < 0.01$). Two-factor ANOVA test revealed that measurement error of stenosis was different between

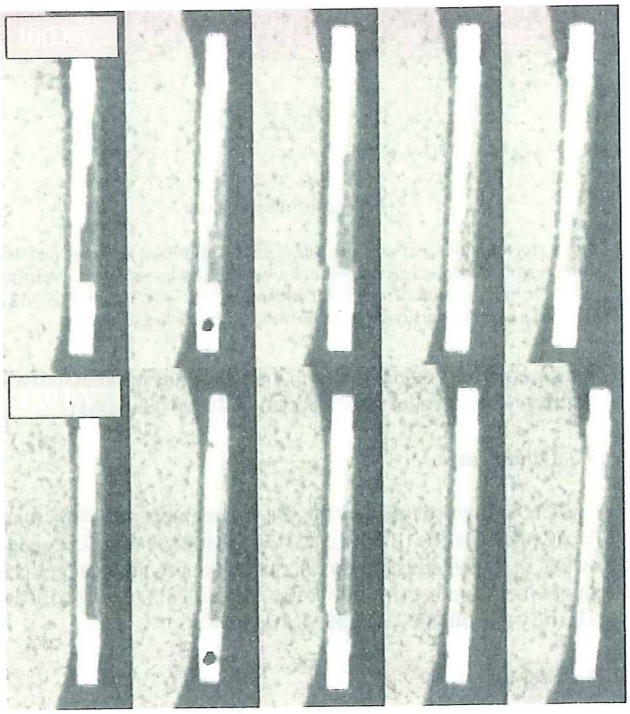

Fig. 3. MPR images of soft plaque models. The MPR images of soft plaque models at 100 kV and 120 kV, under intracoronary enhancement of 205 HU and heart rate of 65 bpm, are shown (window level/width: 600/100). All plaques with three stenosis levels are clearly visualized. Note that delineation of plaques is better at 100 kV due to a large difference in CT values between the plaque and intracoronary enhancement.

Please cite this article in press as: Horiguchi J, et al. In vitro measurement of CT density and estimation of stenosis related to coronary soft plaque at 100 kV and 120 kV on ECG-triggered scan. Eur J Radiol (2009), doi:10.1016/j.ejrad.2009.08.002

Table 3
Plaque densitometry and stenosis measurement by two observers.

	Observer 1, mean ± SD	Observer 2, mean ± SD	Observers 1 and 2		Correlation coefficient
			Bias	Limits of agreement	
Plaque density	23.7 ± 31.2 HU	24.8 ± 29.9 HU	−1.0	−2.7 to 0.7	$r=0.953$, $p<0.0001$
Stenosis measurement	2.0 ± 0.8 mm	2.0 ± 0.8 mm	−0.02	−0.36 to 0.33	$r=0.975$, $p<0.0001$

Interobserver reliability for measurement was tested using Bland–Altman analysis and Pearson correlation coefficient. SD indicates standard deviation.

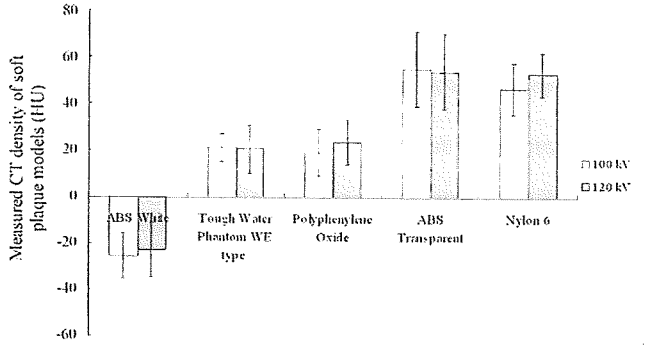

Fig. 4. Measured CT density of soft plaque models. Two-factor ANOVA test revealed that measured CT density of soft plaque models was different between plaque types ($p<0.01$), however, was not between 100 kV and 120 kV ($p=0.24$). Bars and vertical lines show mean and standard deviation. ABS: acrylonitrile–butadiene–styrene.

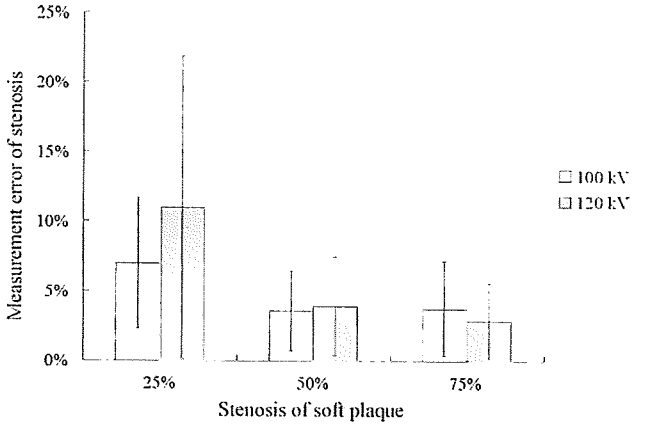

Fig. 5. Measurement error of stenosis. Two-factor ANOVA test revealed that measurement error of stenosis was different between plaque stenosis levels ($p<0.01$), however, did not reach to a statistical difference between 100 kV and 120 kV ($p=0.08$). Bars and vertical lines show mean and standard deviation.

plaque stenosis levels ($p<0.01$), however did not reach to a statistical difference between 100 kV and 120 kV ($p=0.08$) (Fig. 5).

3.3. Radiation dose

The CTDIvol displayed on the CT scanner was 8.51 mGy and 13.72 mGy for the 100 kV and 120 kV prospective ECG-triggered scans. DLPs and effective doses, calculated for a typical patient scan range of 14 cm, were 119.14 mGy cm and 2.03 mSv for 100 kV and 192.08 mGy cm and 3.27 mSv for 120 kV scans.

4. Discussion

The present study is the first to demonstrate that, in slim patients, 100 kV prospective ECG-triggered 64-MDCTA evaluates coronary artery soft plaque comparable to 120 kV in terms of soft plaque densitometry and stenosis measurement, with a reduced effective dose of 2 mSv.

64-MDCTA with retrospective ECG-gating has high assessibility and diagnostic accuracy; however, high radiation is one of most significant problems due to cancerogenic risk [25]. Prospective ECG-triggered technique has shown image quality comparable to retrospective ECG-gated CTA on 64-MDCT [18,19] and dual-source CT [20], as well as equivalent diagnostic accuracy of both acquisitions in comparison using selective coronary angiography as the gold standard [26]. Prospective ECG-triggered technique itself reduces the dose by around 80%. Moreover, to keep to the 'as low as reasonably achievable (ALARA)' strategy, lower tube voltage should be simultaneously applied in appropriate situations, such as to slim and/or small patients.

The use of lower energy photons results in a rapid attenuation increase of elements with high atomic number because of higher photoelectric interactions. Therefore, 100 kV led to higher intracoronary CT values than 120 kV by around 50 HU. In contrast to this, difference in CT values of soft plaque models was small between 100 kV and 120 kV on densitometry with gross samples. In dynamic test simulating coronary CTA, the CT values were different from static measurements and were similar between 100 kV and 120 kV, probably due to partial volume effect and/or motion artifacts. The results seem to suggest two points: (1) real CT value of soft plaque is not precisely assessed in coronary CTA, and (2) although not precise, plaque composition may be speculated based on CT value at 100 kV in a similar way as on the 120 kV scan. A large difference in CT values between soft plaque and coronary artery at 100 kV has other merits; potential reduction of contrast material and assessibility of soft plaque under unexpected decrease of iodine concentration in the coronary artery.

The measurement error of stenosis was different between plaque stenosis levels. A possible explanation for this is due to limited spatial resolution (minimal plaque thickness of 1 mm versus spatial resolution of CT scanner of around 0.6 mm) and the aforementioned fact that densitometry of small plaque is substantially affected by intracoronary enhancement. However, the measurement error of around 5%, in more clinically important 50% or 75% stenosis plaque, seems promising. Interestingly, although not statistically different ($p=0.08$), the measurement error tended to be lower at 100 kV, especially in 25% stenosis plaque. A large difference in CT values between soft plaque and coronary artery may also have an advantage in stenosis measurement of small plaque.

Several limitations of the study should be addressed. The plaque in the study simulated isolated non-calcified plaque, however, most plaque in real life is mixed plaque. Calcium plaque is blurred significantly at lower kV and might obscure soft plaque. Higher heart rates, which may potentially obscure results due to motion artifacts, were not studied. The data is biased with regard to the stenosis since the observers know what stenosis was present before the scan. Ideally, each artery phantom had only one stenosis, and was scanned blindly so that the observers would not know which one was being scanned. The luminal diameter of artery was 4 mm and the situation was only similar to proximal coronary arteries. The low tube voltage entails increasing image noise and for this reason patients with a BMI lower than 25 kg/m^2 were enrolled in previous studies. However, this criterion does not seem consistently rational, as body habitus of the individual patients is not taken into account. Further investigation is needed to establish

Please cite this article in press as: Horiguchi J, et al. In vitro measurement of CT density and estimation of stenosis related to coronary soft plaque at 100 kV and 120 kV on ECG-triggered scan. Eur J Radiol (2009), doi:10.1016/j.ejrad.2009.08.002

more reasonable criteria. For example, image noise measurement on non-contrast CT might be used for the indication for 100 kV.

In conclusion, 100 kV prospective ECG-triggered coronary MDCTA has comparable performance to 120 kV coronary CTA in terms of soft plaque densitometry and measurement of stenosis, with a reduced effective dose of 2 mSv.

Acknowledgement

This study was financially supported by Tsuchiya Foundation (http://www.tsuchiya-foundation.or.jp), Hiroshima, Japan.

References

[1] Narula J, Finn AV, Demaria AN. Picking plaques that pop. J Am Coll Cardiol 2005;45:1970–3.
[2] Little WC, Constantinescu M, Applegate RJ, et al. Can coronary angiography predict the site of a subsequent myocardial infarction in patients with mild-to-moderate coronary artery disease? Circulation 1988;78: 1157–66.
[3] Nissen SE, Yock P. Intravascular ultrasound: novel pathophysiological insights and current clinical applications. Circulation 2001;103:604–16.
[4] Patwari P, Weissman NJ, Boppart SA, et al. Assessment of coronary plaque with optical coherence tomography and high-frequency ultrasound. Am J Cardiol 2000;85:641–4.
[5] Schneiderman J, Wilensky RL, Weiss A, et al. Diagnosis of thin-cap fibroatheromas by a self-contained intravascular magnetic resonance imaging probe in ex vivo human aortas and in situ coronary arteries. J Am Coll Cardiol 2005;45:1961–9.
[6] Stefanadis C, Diamantopoulos L, Vlachopoulos C, et al. Thermal heterogeneity within human atherosclerotic coronary arteries detected in vivo: a new method of detection by application of a special thermography catheter. Circulation 1999;99:1965–71.
[7] Takano M, Mizuno K, Okamatsu K, Yokoyama S, Ohba T, Sakai S. Mechanical and structural characteristics of vulnerable plaques: analysis by coronary angioscopy and intravascular ultrasound. J Am Coll Cardiol 2001;38: 99–104.
[8] Schroeder S, Kopp AF, Baumbach A, et al. Noninvasive detection and evaluation of atherosclerotic coronary plaques with multislice computed tomography. J Am Coll Cardiol 2001;37:1430–5.
[9] Becker CR, Nikolaou K, Muders M, et al. Ex vivo coronary atherosclerotic plaque characterization with multi-detector-row CT. Eur Radiol 2003;13:2094–8.
[10] Viles-Gonzalez JF, Poon M, Sanz J, et al. In vivo 16-slice, multidetector-row computed tomography for the assessment of experimental atherosclerosis: comparison with magnetic resonance imaging and histopathology. Circulation 2004;110:1467–72.
[11] Leber AW, Knez A, Becker A, et al. Accuracy of multidetector spiral computed tomography in identifying and differentiating the composition of coronary atherosclerotic plaques: a comparative study with intracoronary ultrasound. J Am Coll Cardiol 2004;43:1241–7.
[12] Schroeder S, Kuettner A, Leitritz M, et al. Reliability of differentiating human coronary plaque morphology using contrast-enhanced multislice spiral computed tomography. A comparison with histology. J Comput Assist Tomogr 2004;28:449–54.
[13] Nikolaou K, Becker CR, Muders M, et al. Multidetector-row computed tomography and magnetic resonance imaging of atherosclerotic lesions in human ex vivo coronary arteries. Atherosclerosis 2004;174:243–52.
[14] Rasouli ML, Shavelle DM, French WJ, McKay CR, Budoff MJ. Assessment of coronary plaque morphology by contrast-enhanced computed tomographic angiography: comparison with intravascular ultrasound. Coron Artery Dis 2006;17:359–64.
[15] Pohle K, Achenbach S, MacNeill B, et al. Characterization of non-calcified coronary atherosclerotic plaque by multi-detector row CT: comparison to IVUS. Atherosclerosis 2007;190:174–80.
[16] Kitagawa T, Yamamoto H, Ohhashi N, et al. Comprehensive evaluation of non-calcified coronary plaque characteristics detected using 64-slice computed tomography in patients with proven or suspected coronary artery disease. Am Heart J 2007;154:1191–8.
[17] Sun J, Zhang Z, Lu B, et al. Identification and quantification of coronary atherosclerotic plaques: a comparison of 64-MDCT and intravascular ultrasound. AJR 2008;190:748–54.
[18] Hirai N, Horiguchi J, Fujioka C, et al. Prospective electrocardiography-triggered versus retrospective electrocardiography-gated 64-slice coronary CT angiography: image quality, stenoses assessment and radiation dose. Radiology 2008;248:424–30.
[19] Husmann L, Valenta I, Gaemperli O, et al. Feasibility of low-dose coronary CT angiography: first experience with prospective ECG-gating. Eur Heart J 2008;29:191–7.
[20] Stolzmann P, Leschka S, Scheffel H, et al. Dual-source CT in step-and-shoot mode: noninvasive coronary angiography with low radiation dose. Radiology 2008;249:71–80.
[21] Ertl-Wagner BB, Hoffmann RT, Bruning R, et al. Multi-detector row CT angiography of the brain at various kilovoltage settings. Radiology 2004;231: 528–35.
[22] Horiguchi J, Kiguchi M, Fujioka C, et al. Radiation dose, image quality, stenosis measurement, and CT densitometry using ECG-triggered coronary 64-MDCT angiography: a phantom study. AJR 2008;190:315–20.
[23] Horiguchi J, Fujioka C, Kiguchi M, et al. Soft and intermediate plaques in coronary artery: how accurately can we measure CT density by 64-slice CT? AJR 2007;189:981–8.
[24] European Guidelines on Quality Criteria for Computed Tomography. Available at http://www.drs.dk/guidelines/ct/quality/index.htm. Accessed December; 2008.
[25] Einstein JA, Henzlova MJ, Rajagopalan S. Estimating risk of cancer associated with radiation exposure from 64-slice computed tomography coronary angiography. JAMA 2007;298:317–23.
[26] Maruyama T, Takada M, Hasuike T, et al. Radiation dose reduction and coronary assessability of prospective electrocardiogram-gated computed tomography coronary angiography. J Am Coll Cardiol 2008;52:1450–5.

Please cite this article in press as: Horiguchi J, et al. In vitro measurement of CT density and estimation of stenosis related to coronary soft plaque at 100 kV and 120 kV on ECG-triggered scan. Eur J Radiol (2009), doi:10.1016/j.ejrad.2009.08.002

Current Cardiac Imaging Reports, 2010 in press.

Prospective Electrocardiograph (ECG)-triggered Sequential Versus Retrospective ECG-Gated Spiral Computed Tomography: Pros and Cons

Jun Horiguchi, MD [1)] horiguch@hiroshima-u.ac.jp
Hideya Yamamoto, MD [2)] hideyayama@hiroshima-u.ac.jp
Yasuki Kihara, MD Prof [2)] ykihara@hiroshima-u.ac.jp
Katsuhide Ito, MD Prof [3)] hidechan@hiroshima-u.ac.jp

1) Department of Clinical Radiology, Hiroshima University Hospital
Address: 1-2-3, Kasumi-cho, Minami-ku, Hiroshima, 734-8551, Japan

2) Department of Molecular and Internal Medicine, Division of Clinical Medical Science, Programs for Applied Biomedicine, Graduate School of Biomedical Sciences, Hiroshima University
Address: 1-2-3, Kasumi-cho, Minami-ku, Hiroshima, 734-8551, Japan

3) Department of Radiology, Division of Medical Intelligence and Informatics, Programs for Applied Biomedicine, Graduate School of Biomedical Sciences, Hiroshima University
Address: 1-2-3, Kasumi-cho, Minami-ku, Hiroshima, 734-8551, Japan

Corresponding author:
Jun Horiguchi, MD
Tel: +81 82 2575257, Fax: +81 82 2575259
E-mail: horiguch@hiroshima-u.ac.jp

Abstract

Advancement of multidetector computed tomography (CT) makes it possible to visualize coronary artery as well as assessing ventricular and valvular motion, however, the necessary radiation dose is higher than that associated with X-ray coronary angiography. Recently introduced prospective electrocardiograph (ECG)-triggered CT angiography (CTA), using conventional axial scan, can markedly reduce the radiation dose, while maintaining diagnostic performance, as far as appropriately applied to selected patients. The prospective ECG-triggered CTA is technically feasible to patients with low and stable heart rate. The suitable indication is exclusion of obstructive coronary disease, rather than the analyzing of ventricular and valvular function. The scan is most beneficial for young patients, especially young women, who are at low risk of significant coronary artery disease and for whom radiation dose is of great concern.

Introduction

The diagnostic accuracy of retrospective ECG-gated 64-slice CTA, compared to coronary angiography as golden standard, is demonstrated to be high by both meta analysis [1] and prospective multicenter studies [2,3]. The major merits of this technique are low invasiveness and high negative predictive value to rule out obstructive coronary artery stenosis. This can reduce invasive coronary angiography for purely diagnostic purpose. The high radiation exposure however, being related to increasing cancerogenic risk, is a serious concern [4].

Recently introduced prospective ECG-triggered CTA, reducing radiation dose by around 80%, is gaining interest. In this article, we describe technique, radiation and associated risk, diagnostic performance and indication of prospective ECG-triggered CTA, compared to retrospective ECG-gated CTA.

1. Technical Issues

1-1. Navigator for Respiratory and Cardiac Motion

Two sources of motion, i.e. respiratory and cardiac contraction/relaxation, are associated with cardiac imaging. If the image acquisition time is longer than the patient's ability of breath-hold time, respiratory movement should be suppressed by respiratory-gating. For

typical magnetic resonance coronary angiography, navigator echoes are used to track patient's diaphragmatic motion during free-breathing. In contrast, if the data acquisition is performed within duration of one breath-hold, typically in contrast-enhanced first-pass imaging, both magnetic resonance coronary angiography and CTA (always) are obtained during a breath-hold. In this situation, ECG is mainly used in order to reduce motion artifacts from the heart (kymogram as an alternative).

1-2. Prospective ECG-triggered versus Retrospective ECG-gated Techniques

For images free of cardiac motion artifacts, acquisition times shorter than 19.1 msec are necessary [5]. Neither multidetector or electron beam CT has such a high temporal resolution, thus imaging of the heart on CT needs to appropriately fit the scan window to relatively stable timing of the heartbeat. According to Lu [6], by optimization of the cardiac phase using ECG-triggering/gating, cardiac images with the least-motion can be obtained with an acquisition time of 50-70 msec for a patient baseline heart rate of 50-100 beats per minute (bpm).

In coronary CTA, prospective ECG-triggered technique, which exposes X-ray only at a predetermined cardiac phase (usually diastolic) has been used from earlier-generation electron beam CT scanner (C-100XL, C-150XL), while the major application of this scanner is coronary artery calcium scoring. From the introduction of multidetector CT (typically 4-slice), retrospective ECG-gating, which continuously exposes X-ray with simultaneous ECG-information acquisition, thereafter, data for specific cardiac phase are used for image reconstruction, has been the mainstream in coronary CTA. Sixty-four-slice CT, and 256 or 320-slice CT, by virtue of increased coverage in the z-axis and improved temporal resolution, are drawing attention to reconsider prospective ECG-triggering.

Conventional retrospective ECG-gated scan is performed in the spiral mode using a fixed tube current throughout the cardiac cycle (Fig. 1A) and later the images are reconstructed at a specific cardiac phase(s). Depending on CT scanners, the phase(s) are quoted as a percentage of the RR interval (e.g. 75%) or as a value of absolute delay (e.g. 700msec). The cardiac phase with the least motion artifacts is known to vary for each coronary artery and between patients. In general, mid- or late-diastolic phase provides (almost) motion-free coronary artery images in low heart rate (i.e. <65 bpm). However, reconstruction at late-systolic phase becomes necessary in a higher heart rate. Searching the best phase for each coronary artery from among several phases (images are often reconstructed at 5% of RR interval) is time-consuming and effortful. For an automatic

technique, the 'Motion maps', which derives a motion strength function between multiple low-resolution reconstructions through the cardiac cycle, with periods of lowest difference between neighboring phases indicating minimal cardiac motion, has an advantage [7]. Apart from coronary artery imaging, retrospective ECG-gated scan can evaluate global and regional cardiac function (i.e. ejection fraction) and valvular morphology and function (Figure 2). Retrospective ECG-gated scan can accommodate mildly irregular heart rhythm. Using ECG-editing technique, one can arbitrarily modify the position of the temporal windows within the cardiac cycle, and correct and compensate for part or all of the artifacts produced by heart rhythm irregularities [8] (Figure 3). Thus, through data covering the entire cardiac phase, retrospective ECG-gated scan has availability in multicardiac phase reconstruction and also has the robustness for mild heart rate variation.

As a modification to conventional retrospective ECG-gated scan, current multidetector CT scanners have the option so called 'ECG-modulation', which modulates the tube current during a particular part of the cardiac cycle (Fig. 1B), allowing reduction of the radiation dose by 30% to 50% [9,10]. The extent of reduction depends on the setting of two parameters; (1) percentage of minimum tube current /maximum tube current and (2) the length of time with the minimal tube current relative to the RR interval. Systolic phase, which is not usually used in coronary artery imaging, is chosen for window at reduced current. However, cardiac function can be reasonably assessed as such high image quality in the systole is not demanded.

Prospective ECG-triggered technique, which applies radiation during short and predefined acquisition window of the cardiac cycle, has recently been devised. The R wave on the ECG is monitored; the scan starts following a time delay and stops after a certain period to resume at a similar time during the next cycle (Fig. 1C). Therefore, the image quality inherently degrades in cases of entopic beat or other arrhythmia. On 64-slice CT, step-and-shoot technique (around 4 shoots) is used to cover the entire heart. Between the adjacent X-ray exposures, one heartbeat is usual for table movement, except for low heart rate (e.g. < bpm), in which the table can move during X-ray-off time (systole). Regarding a disadvantage of 64-slice prospective ECG-triggered CTA, stair-step artifact, by incorrect fusion of two adjacent datasets, potential occurs and can be a reason for 'non-diagnostic' evaluability of coronary artery [11]. This can occur due to both heart rate instability and body movement. In this respect, 256 or 320-slice CT, allowing for a one-heartbeat-scan, has a definite advantage.

At least 180° of parallel-ray projections are needed to reconstruct an image. A single-source CT scanner needs half a rotation plus the fan angle (about 50° to 60°) to

deliver this amount of data, and the temporal resolution in the center of rotation is half the rotation time [12]. To reduce the radiation dose to the minimum, the least gantry rotation (230° to 240°) is used, while imaging is limited to only one cardiac phase. To accommodate some heart rate variation or to acquire broad phase data (e.g. end-systole to late-diastole) or even acquire two cardiac-cycle data (for multisegment reconstruction), one can elongate exposure time at the expense of increased radiation exposure (Fig. 1D). Some issues related to this technique remain unresolved. Most practitioners are unfamiliar with the optimal setting for X-ray exposure duration (minimal exposure time + safety margin) due to paucity of data or consensus. The optimal duration depends on several factors; (1) patient's heart rate and variation, (2) purpose of cardiac exam (coronary artery imaging or including functional analysis), (3) different gantry rotation speeds (0.27 to 0.35 sec/rotation) affecting the temporal resolution. Although complicated, to simplify and generalize this matter for practical guidance, we support adding 50 msec to the minimal exposure for coronary artery imaging, recommended by Kimura [13]. The capability in the elongation of exposure duration is different from CT scanners. Functional imaging or multi-segment reconstruction using two adjacent cardiac cycles becomes possible if the exposure duration can be set long enough. Apart from single-source CT scanner, dual-source CT, embedded with two acquisition systems mounted at an angular offset of 90° on the rotating gantry, 180° of parallel-ray geometry data can be split into two data segments of 90°. Both 90° data segments are acquired simultaneously at the same anatomical level within a quarter of the gantry rotation time (330 msec), thereby the temporal resolution is 83msec. When applying multi-segment reconstruction, the temporal resolution of 41 to 83 msec (average, 60msec) can be achieved [12].

2. Radiation Exposure

2-1. Risk Estimate

The additional lifetime risk of fatal cancer has been estimated as approximately 1 in 20,000 per mSv for the whole population by The International Commission on Radiological Protection [14]. This is also supported by The Food and Drug Administration [15]. The recent Biological Effects of Ionizing Radiation (BEIR) VII Phase 2 report [16] provided a framework for estimating lifetime attributable risk (LAR) of cancer incidence associated with radiation exposure from cardiac multidetector CT and indicated that a single population dose of 10 mSv is associated

with a LAR for developing a solid cancer or leukaemia of 1 in 1000. Therefore, CT scan needs to keep the radiation exposure "as low as reasonably achievable (ALARA)".

2-2. Radiation Exposure of Cardiac Examination

The effective doses of various CT scanners and protocols, as well as other diagnostic modalities [10,11,17-32] for comparison, are listed in Table 1. In the tradeoff of improved diagnostic capability by virtue of advances in the spatial and temporal resolution of spiral CT scanners, the radiation dose of cardiac CT examinations has increased from 4-slice to 64-slice CT. The effective dose of non-ECG-modulated 64-slice CT is high (15.2-21.4), as a commonly used pitch of 0.2 results in 80% overlap.

2-3. How to Reduce Radiation Exposure in Cardiac CT

As described earlier, ECG-modulation on retrospective ECG-gated CTA (30-50% reduction) and the use of prospective ECG-triggered CTA (77-83% reduction compared to ECG-modulated retrospective ECG-gated CTA) [24-27] are two major solutions. Low tube voltage is also effective as the radiation dose varies with the square of the kilovoltage. Decreased tube voltage increases image noise, however leads to increased opacification of vascular structures during contrast-enhanced CTA owing to an increase in the photoelectric effect and a decrease in Compton scattering [33]. Abada et al. used a tube voltage of 80 kV for 64-slice CTA and reported a dose saving of up to 88% [34]. The combination of prospective ECG-triggered CTA and 100 kV in selected patients (typically body mass index [BMI] < 25 kg x m^{-2}) succeeds in a marked reduction of radiation exposure in 64-slice CTA [11, 27-29] or dual-source CTA [30,31].

The automatic exposure control can optimize and reduce tube current. The cross section of the human body differs significantly from a circular shape, thus the attenuation of X-ray beams vary. The new online tube current modulation system takes this fact into account and automatically adjusts tube current in the x, y plane (angular modulation) or along z-axis direction, or both (combined modulation) in order to obtain constant image quality. Deetjen reported that this technique reduced the dose by 42.8% [35].

Other techniques include minimizing scan range and reducing field of view.

3. Diagnostic Performance of Prospective ECG-triggered Scan

Clinical importance of coronary CTA, which is based on evidence on retrospective ECG-gated CTA, is reported in detail elsewhere [36]. Here, we focus on the performance of prospective ECG-triggered scan.

3-1. Prospective ECG-triggered versus Retrospective ECG-gated Techniques

On 64-slice CT, a phantom study shows that prospective ECG-triggered and retrospective ECG-gated CTA have comparable performance in terms of image quality, stenosis measurement, and CT densitometry on stable heart rates up to 75 bpm [37]. The similarity on image quality and stenosis measurement has been shown in a study with the same patients' group with a heart rate < 75 bpm [24]. In different patients' groups also, image quality was reported to be similar in < 75 bpm [25]. Earls reported that prospective ECG-triggered revealed improved image quality and similar coronary artery assessability, with a heart rate < 70 pm and fluctuation < 10bpm prior to the scan [27].

Representative images on the two scan techniques obtained from the same patient are shown (Figure 4A). Prospective ECG-triggered technology is still its infancy thus there are few reports on stent imaging. In our early experience, the image quality on the two scan techniques seems to be comparable (Figure 4B). Prospective ECG-triggered scan may sometimes be advantageous as this is not inherently related to helical artifacts.

On dual-source CTA, Alkadhi reported that diagnostic image quality was obtained in around 98% of coronary artery segments (≤ 70bpm) on prospective ECG-triggered scan, which was not different from the prevalence on retrospective ECG-gated scan (> 70 bpm).

3-2. Prospective ECG-triggered versus Invasive Angiography

Similar to reported results on retrospective ECG-gated CTA, initial prospective ECG-triggered CTA studies, in selected patients with low and regular heart rate, have shown accurate diagnosis of significant (≥50%) coronary stenosis with almost 100% negative predictive value on both 64-slice CT [26,28] and dual-source CT [29] (Figure 5). It is, however, too early to conclude the value of prospective ECG-triggered CTA therefore collection of data in larger cohorts is needed.

4. Indication of Prospective ECG-triggered CTA

4-1. Technical Indication

Due to the nature of prospective ECG-triggering, scanning requires patients having a stable sinus rhythm and low heart rate [28]. The indication is considered to become stricter when we shorten X-ray exposure duration. Husmann showed that, using receiver operator characteristic curve, only 1% of coronary segments were non-diagnostic below a heart rate of 63 bpm, whereas 14.8% with heart rate of > 63 bpm ($p < 0.001$).

Although using higher temporal resolution (83 msec) on dual-source CT scanner, strict heart rate indication has been suggested. Scheffel stated that prospective ECG-triggering was feasible in selected patients with regular heart rates below 70 bpm and allows for the depiction of 98% of the coronary segments with diagnostic image quality [29]. Stolzmann showed that receiver operator characteristic analyses revealed a mean heart rate threshold for the prediction of motion artifacts of 59.9 bpm and a heart rate variability threshold for the prediction of stair-step artifacts of 2.2 bpm [30]. Gutstein recommend the indication for patients with heart rate < 65 or 70 bpm (depending on a coronary artery calcium score < or ≥ 400 HU) and a maximal heart rate variation before CTA of < 10 bpm [38].

Thus, successful prospective ECG-triggering CTA largely depends on a patient's heart rate and variability. Control of heart rate should be strict and the use of heart rate lowering drugs, such as beta blockers should be encouraged, unless contraindicated.

4-2. Clinical Indication

To reduce the radiation exposure in prospective ECG-triggered CTA, the available cardiac phase(s) would be minimized (e.g. single phase). Single-phase prospective ECG-triggered CTA appears to be the most suitable for young patients, especially young women, who are at low risk of significant coronary artery disease and in whom radiation dose is of great concern. Such a protocol might be considered appropriate as an alternative to coronary calcium scanning in circumstances in which the earliest detection of coronary atherosclerosis is desired [38].

5. Limitations of coronary CTA and Advantage of Prospective ECG-triggered CTA

According to a recent statement [36], limitations of coronary CTA include; (1) Calcifications within the coronary arteries can cause false negatives and, more frequently, false-positive findings concerning the presence of coronary artery stenosis.

(2) Coronary artery segments with substantial calcification may not be evaluable with respect to the presence of a hemodynamically relevant stenosis. (3) The coronary lumen is generally not well observed in the region of a coronary stent. In addition to these, the adverse effect of iodinated contrast media and risk for radiation exposure are common problems related to contrast-enhanced CT. The latter is highlighted in low-pitch helical mode cardiac CTA. Prospective ECG-triggered CTA, with low radiation exposure, is promising and any efforts to further optimize or reduce the dose should be made.

Conclusion

Prospective ECG-triggered CTA can markedly reduce the radiation dose, while maintaining diagnostic performance, in patients with low and stable heart rate. The suitable indication is exclusion of obstructive coronary disease and is most beneficial for young patients, who are at low risk of significant coronary artery disease.

Abbreviations

ECG: electrocardiograph
CT: computed tomography
CTA: computed tomography angiography
bpm: beats per minute
BMI: body mass index

References and Recommended Reading

Papers of particular interest, published recently, have been highlighted as:

* Of importance

** Of major importance

1. Abdulla J, Abildstrom SZ, Gotzsche O, et al. **64-multislice detector computed tomography coronary angiography as potential alternative to conventional coronary angiography: a systematic review and meta-analysis.** European Heart Journal 2007;28:3042-3050.

2. Budoff MJ, Dowe D, Jollis JG, et al. **Diagnostic performance of 64-multidetector row coronary computed tomographic angiography for evaluation of coronary artery stenosis in individuals without known coronary artery disease.** JACC 2008;52:1724-1732.

3. Meijboom WB, Meijs MF, Schuijf JD, et al. **Diagnostic accuracy of 64-slice computed tomography coronary angiography. a prospective, multicenter, multivendor study.** J Am Coll Cardiol 2008;52:2135-2144.

4. Einstein AJ, Moser KW, Thompson RC, et al. **Radiation dose to patients from cardiac diagnostic imaging.** Circulation 2007;116:1290-1305.

5. Ritchie CJ, Godwin JD, Crawford CR, et al. **Minimum scan speeds for suppression of motion artifacts in CT.** Radiology 1992;185:37-42.

6. Lu B, Mao SS, Zhuang N, et al. **Coronary artery motion during the cardiac cycle and optimal EKG triggering for coronary artery imaging.** Invest Radiol 2001;36:250-256.

7. Hoffmann MHK, Lessick J, Manzke R et al. **Automatic determination of minimal cardiac motion phases for computed tomography imaging: initial experience.** Eur Radiol 2006;16:365-373.

8. Cademartiri F, Mollet NR, Runza G, et al. **Improving diagnostic accuracy of MDCT coronary angiography in patients with mild heart rhythm irregularities using ECG editing.** AJR 2006;186:634-638.

9. Jakobs TF, Becker CR, Ohnesorge B, et al. **Multislice helical CT of the heart with retrospective ECG gating: reduction of radiation exposure by ECG-controlled tube current modulation.** Eur Radiol 2002;12:1081-1086.

10. Hausleiter J, Meyer T, Hadamitzky M, et al. **Radiation dose estimates from cardiac multislice computed tomography in daily practice: impact of different scanning protocols on effective dose estimates.** Circulation 2006;113:1305-1310.

11. Husmann L, Valenta I, Gaemperli O, et al. **Feasibility of low-dose coronary CT**

angiography: first experience with prospective ECG-gating. European Heart Journal 2008;**29**;191-197.
12. Petersilka M, Bruder H, Krauss B, Stierstorfer K, Flohr TG. **Technical principles of dual source CT.** European Journal of Radiology 2008;**68**:362-368.
13. Kimura F, Umezawa T, Shen Y, et al. **Coronary CT angiography using prospectively gated axial scans: evaluation of banding artifacts and padding time.** Presented at Radiological Society of North America 2008.
14. 1990 recommendations of the International Commission on Radiological Protection. ICRP Publication 60. Ann ICRP 1990;21
15. US Food and Drug Administration Center for Devices and Radiological Health. Whole body scanning using computed tomography (CT): what are the radiation risks from CT? Available at: www.fda.gov/cdrh/ct/risks.html. Accessed January 2009.
16. Committee to assess health risks from exposure to low levels of ionizing radiation, National Research Council. Nuclear and Radiation Studies Board. Health risks from exposure to low levels of ionizing radiation.2005. 2006. Washington, DC, The National Academies Press. Ref Type: Report.
17. Morin RL, Gerber TC, McCollough CH. **Radiation dose in computed tomography of the heart.** Circulation 2003;**107**:917-922.
18. Einstein AJ, Moser KW, Thompson RC, et al. **Radiation dose to patients from cardiac diagnostic imaging.** Circulation 2007;**116**:1290-1305.
19. Hunold P, Vogt FM, Schmermund A, et al. **Radiation exposure during cardiac CT: effective doses at multi-detector row CT and electron-beam CT.** Radiology 2003;**226**:145-152.
20. Achenbach S, Giesler T, Ropers D, et al. **Detection of coronary artery stenoses by contrastenhanced, retrospectively electrocardiographically-gated, multislice spiral computed tomography.** Circulation 2001;**103**:2535-2538.
21. Mollet NR, Cademartiri F, van Mieghem CA, et al. **High-resolution spiral computed tomography coronary angiography in patients referred for diagnostic conventional coronary angiography.** Circulation **2005**;112:2318–23.
22. Oncel D, Oncel G, Tastan A. **Effectiveness of dual-source CT coronary angiography for the evaluation of coronary artery disease in patients with atrial fibrillation: initial experience.** Radiology 2007;**249**:703-711.
23. Stolzmann P, Scheffel H, Schertler T, et al. **Radiation dose estimates in dual-source computed tomography coronary angiography.** Eur Radiol 2008;**18**:592-599.
24. * Hirai N, Horiguchi J, Fujioka C, et al. **Prospective**

electrocardiography-triggered versus retrospective electrocardiography-gated 64-slice coronary CT angiography: image quality, stenoses assessment and radiation dose. Radiology 2008;248:424-430.
This study shows the comparability of prospective ECG-triggered to ECG-modulated retrospective ECG-gated 64-slice CTA as regards image quality and stenoses assessment in the same patients (n=60), while dose reduction by 79%.
25. Shuman WP, Branch KR, May JM, et al. **Prospective versus retrospective ECG gating for 64-detector CT of the coronary arteries: comparison of image quality and patient radiation dose.** Radiology 2008;248:431-437.
26. ** Maruyama T,Masanori Takada M, et al. **Radiation dose reduction and coronary assessability of prospective electrocardiogram-gated computed tomography coronary angiography.** J Am Coll Cardiol 2008;52:1450-1455.
An important study shows that prospective ECG-triggered 64-slice CTA (n=76) has equivalent coronary assessability and diagnostic accuracy in comparison with ECG-modulated retrospective ECG-gated CTA (n=97) with decreased radiation dose by 79% reduction.
27. Earls JP, Berman EL, Urban BA, et al. **Prospectively gated transverse coronary CT angiography versus retrospectively gated helical technique: improved image qualityand reduced radiation dose.** Radiology 2008; 246:742-753.
28. Herzog BA, Husmann L, Burkhard N, et al. **Accuracy of low-dose computed tomography coronary angiography using prospective electrocardiogram-triggering: first clinical experience.** European Heart Journal 2008;29:3037-3042.
29. * Scheffel H, Alkadhi H, Leschka S, et al. **Low-dose CT coronary angiography in the step-and-shoot mode: diagnostic performance.** Heart 2008;94:1132-1137.
This article investigates the diagnosis of significant coronary artery disease on prospective ECG-triggered dual-source CTA in 120 patients, compared to invasive angiography.
30. Stolzmann P, Leschka S, Scheffel H, et al. **Dual-source CT in step-and-shoot mode: noninvasive coronary angiography with low radiation dose.** Radiology 2008; 249: 71-80.
31. Alkadhi H, Stolzmann P, Scheffel H, et al. **Radiation dose of cardiac dual-source CT: the effect of tailoring the protocol to patient-specific parameters.** European Journal of Radiology 2008;68:385-391.
32. Rybicki FJ, Otero HJ, Steigner ML, et al. **Initial evaluation of coronary images from 320-detector row computed tomography.** Int J Cardiovasc Imaging

2008;24:535-546.
33. Ertl-Wagner BB, Hoffmann RT, Bruning R, et al. **Multi-detector row CT angiography of the brain at various kilovoltage settings.** Radiology 2004;231:528-535.
34. Abada HT, Larchez C, Daoud B, et al. **MDCT of the coronary arteries: feasibility of low-dose CT with ECG-pulsed tube current modulation to reduce radiation dose.** AJR 2006;186:S387-390.
35. Deetjen A, Mo¨llmann S, Conradi G, et al. **Use of automatic exposure control in multislice computed tomography of the coronaries: comparison of 16-slice and 64-slice scanner data with conventional coronary angiography.** Heart 2007;93:1040-1043.
36. Bluemke DA, Achenbach S, Budoff M, et al. **Noninvasive coronary artery imaging: magnetic resonance angiography and multidetector computed tomography angiography: a scientific statement from the American Heart Association Committee on Cardiovascular Imaging and Intervention of the Council on Cardiovascular Radiology and Intervention, and the Councils on Clinical Cardiology and Cardiovascular Disease in the Young.** Circulation 2008;118:586-606.
37. Horiguchi J, Kiguchi M, Fujioka C, et al. **Radiation dose, image quality, stenosis measurement, and CT densitometry using ECG-triggered coronary 64-MDCT angiography: a phantom study.** AJR 2008;190:315-320.
38. Gutstein A, Wolak A, Lee C, et al. **Predicting success of prospective and retrospective gating with dual-source coronary computed tomography angiography: development of selection criteria and initial experience.** J Cardiovasc CT 2008;2:81-90.

Table

Effective Dose of Cardiac Examination

Diagnostic modality	Effective dose (mSv)	Reference No.
Radioisotope		
Diagnostic coronary angiogram	3–10*	17
99mTc sestamibi rest-stress	11.3*	18
99mTc sestamibi stress only	7.9*	18
201Tl stress-redistribution	22*	18
201Tl stress-reinjection	31.4*	18
Dual isotope 201Tl-99mTc sestamibi	29.2	
Calcium Scoring with Electron-Beam CT	1-1.3	19
Retrospective ECG-gated CTA		
4-slice CTA	3.9-5.8	20
64-slice CTA	15.2–21.4	21
Dual-source CT	13.8	22
ECG-modulated 64-slice CTA	9	10
ECG-modulated dual-source CT	7-9	23
Prospective ECG-triggered CTA		
Electron beam CTA	1.5-2	19
64-slice CTA	4.1-4.3	24-26
64-slice CTA (100 kV and 120 kV)	2.1-2.8	11, 27-29
Dual-source CTA	2.6-2.9	30,31
Dual-source CTA, 100 kV	1.2-1.3	30,31
320-slice CTA	6.8**	32

* The effective dose estimated from tissue dose coefficients, using ICRP Publication 60 tissue weighting factors.

** The phase window was set to 60–100% of RR interval.

Figure legends

Figure 1 Prospective ECG-triggered versus Retrospective ECG-gated Techniques

A: Conventional retrospective ECG-gated scan is performed in the spiral mode using a fixed tube current throughout cardiac cycle.
B: ECG-modulated retrospective ECG-gated scan reduces the tube current during a particular part of the cardiac cycle (usually systole), allowing for a reduction of the radiation dose by 30% to 50%.
C: Prospective ECG-triggered scan applies radiation during short and predetermined acquisition window of the cardiac cycle, thereby reducing the radiation dose by around 80%, compared to the retrospective ECG-gated scan.
D: X-ray exposure in prospective ECG-triggered scan can be elongated to increase additional reconstruction availability. It enables the accommodation of some heart rate variation, however, at the expense of increased radiation exposure.

Figure 2 Wall Motion Evaluation on Retrospective ECG-gated Technique

59 yo female with previous history of myocardial infarction
Upper panels show two-chambers view and lower three-chambers view. Left panels indicate diastolic phase and right systolic. The apicoseptal wall shows thinning and endocardial fat deposition, associated with segmentally decreased wall motion. The wall of the proximal right coronary artery is calcified and the lumen is not enhanced.

Figure 3 ECG Editing Technique

The heart rate with a patient presenting arrhythmia ranged 34 to 145 bpm. The reconstruction at 75% of RR shows marked stair-step (i.e. banding) artifacts (left panel). The image misregistration is reduced after applying ECG-editing technique (right).

Figure 4 Comparison of Prospective ECG-triggered versus Retrospective ECG-gated Images

A: 78 yo male complaining of recent myocardial infarction (Agatston score: 350 units). Prospective ECG-triggered (left panel, 60 bpm) and retrospective ECG-gated (right, 61 bpm) images show comparable image quality.
B: 65 yo male, with 3.5mm DRIVER stent implanted in the left main coronary artery, complaining of indeterminate chest pain.
Similarly on both scans (prospective ECG-triggered; left panel, 57 bpm, retrospective ECG-gated; right, 58 bpm), the patency of the stent can be confirmed on curved multiplanar reconstruction views along long and short axes of the stent.

Figure 5 Comparison of Prospective ECG-triggered and Retrospective ECG-gated Images versus Invasive Angiography

62 yo male complaining of progressive effort angina
Curved multiplanar reformation images of prospective ECG-triggered (left panel) and retrospective ECG-gated (middle) images show severe stenosis caused by complex (calcified and non-calcified) plaque. Angiography shows 90% stenosis at the proximal right coronary artery.